STUK

STUK-YTO-TR 159 November 1999

FIRE SPREAD SIMULATION OF A FULL SCALE CABLE TUNNEL

Risto Huhtanen
VTT Energy

In STUK this report was supervised by **Jouko Marttila**

STUK • SÄTEILYTURVAKESKUS • STRÅLSÄKERHETSCENTRALEN
RADIATION AND NUCLEAR SAFETY AUTHORITY

The conclusions presented in the STUK report series are those of the authors and do not necessarily represent the official position of STUK.

ISBN 951-712-348-5
ISSN 0785-9325

Oy Edita Ab, Helsinki 1999

HUHTANEN Risto (VTT Energy). Fire spread simulation of a full scale cable tunnel. STUK-YTO-TR 159. Helsinki 1999. 27 pp.

ISBN 951-712-348-5
ISSN 0785-9325

Keywords: cable fire, simulation, tunnel

ABSTRACT

A fire simulation of a full scale tunnel was performed by using the commercial code FLUENT as the simulation platform. Estimation was made for fire spread on the stacked cable trays, possibility of fire spread to the cable trays on the opposite wall of the tunnel, detection time of smoke detectors in the smouldering phase and response of sprinkler heads in the flaming phase.

According to the simulation, the rise of temperature in the smouldering phase is minimal, only of the order 1 °C. The estimates of optical density of smoke show that normal smoke detectors should give an alarm within 2–4 minutes from the beginning of the smouldering phase, depending on the distance to the detector (in this case it was assumed that the thermal source connected to the smoke source was 50 W). The flow conditions at smoke detectors may be challenging, because the velocity magnitude is rather low at this phase. At 4 minutes the maximum velocity at the detectors is 0.12 m/s.

During the flaming phase (beginning from 11 minutes) fire spreads on the stacked cable trays in an expected way, although the ignition criterion seems to perform poorly when ignition of new objects is considered. The upper cable trays are forced to ignite by boundary condition definitions according to the experience found from a full scale experiment and an earlier simulation. After 30 minutes the hot layer in the room becomes so hot that it speeds up the fire spread and the rate of heat release of burning objects. Further, the hot layer ignites the cable trays on the opposite wall of the tunnel after 45 minutes.

It is estimated that the sprinkler heads would be activated at 20–22 minutes near the fire source and at 24–28 minutes little further from the fire source when fast sprinkler heads are used. The slow heads are activated between 26–32 minutes.

CONTENTS

1 INTRODUCTION

In this paper a fire simulation of a cable tunnel is presented. The work is connected with safety aspects of Finnish nuclear power plants but the same method should be applicable to other cable installations as well.

The purpose of the analysis is to find out the smoke spread in a tunnel in the smouldering phase of a fire and after that to simulate the fire spread in the flaming phase. In the smouldering phase the main interest is in the optical smoke density at the smoke detectors. The alarm is triggered after two detectors, located 6 m from each other, indicate smoke.

The temperature and radiation fields at the times of smoke detection and sprinkler head activation are given in order to make a rough estimate of the cable damage at that time.

In the simulation of the smouldering phase the fire source is given as a smoke and heat input. The beginning of the flaming phase is given as an input rather than predicted by the model.

In the flaming phase the fire spread and fuel pyrolysis is calculated with a model described in [1] in which it has been tested against a full scale cable fire experiment [2]. In the experiment the cross section of the tunnel was similar to the cross section used here. The fire spread and pyrolysis model relies on experimental data given by cone calorimeter tests. The present simulation represents the actual practical case found on any power plant.

Smoke spread simulation has been studied in reference [3] in which the simulated smoke density is compared with the measurements. The detector response is given in references [4] and [5] where several smoke detectors were tested in full scale experiments.

2 GRID AND BOUNDARY CONDITIONS

The domain considered is a cable tunnel which has features found for example in the cable tunnels of TVO power plant in Olkiluoto. The cross section is similar to the tunnels found in that plant. The general layout of a cable tunnel is given in Figure 1. The modelled case is somewhat simplified from this. The tunnel is modelled as a straight one. The left end of the modelled tunnel is closed and the right end opening is described with an open hole at the end of the tunnel.

The cross section of the tunnel is presented in Figure 2. The cable trays are located at heights 1.5 m, 1.8 m and 2.1 m from the tunnel floor. Other trays may be found in the real tunnel, but only these six are taken into account in the simulation. The fire starts from tray C1, first as a smouldering fire and then developing to flaming phase. The trays are modelled with three cells in the vertical direction with thin surface cells in order to capture both the surface temperature and heat capacity of the cable material.

The tunnel walls are of concrete. The heat capacity of the walls is taken into account by using conducting solid cells in part of the domain and fixed temperature surfaces far from the fire source at the ends of the tunnel.

The computational domain and structures are presented in Figure 3. The cable trays are modelled only in the middle part of the tunnel. The number of computational cells in the whole domain is 114 345 of which 76 146 are in the fluid part. Other cells are used for boundary conditions and structures.

The flow field is solved in the domain together with temperature, turbulence and species equations for combustion with the FLUENT code. Radiative heat transfer is calculated using discrete transfer method. In addition, a scalar equation is used to calculate the smoke mass concentration in the volume. Due to its limitations, the soot model of FLUENT can not be used for this purpose. The soot model is used for calculating local absorption coefficients for radiative heat transfer. All the models used for fluid flow and heat transfer are standard options in FLUENT package [6].

For the best numerical accuracy the second

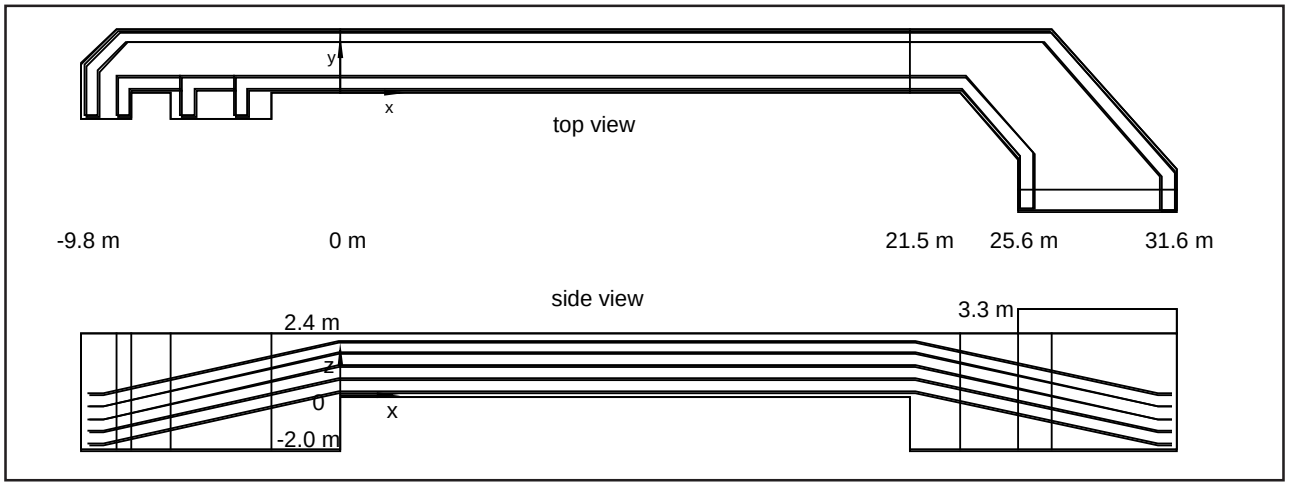

Figure 1. *A general layout of a cable tunnel found in a power plant. The left end of the tunnel is closed, the right end is open to other rooms. The cross section of the tunnel is 2.4 m × 2.4 m. The cable trays are 0.5 m wide.*

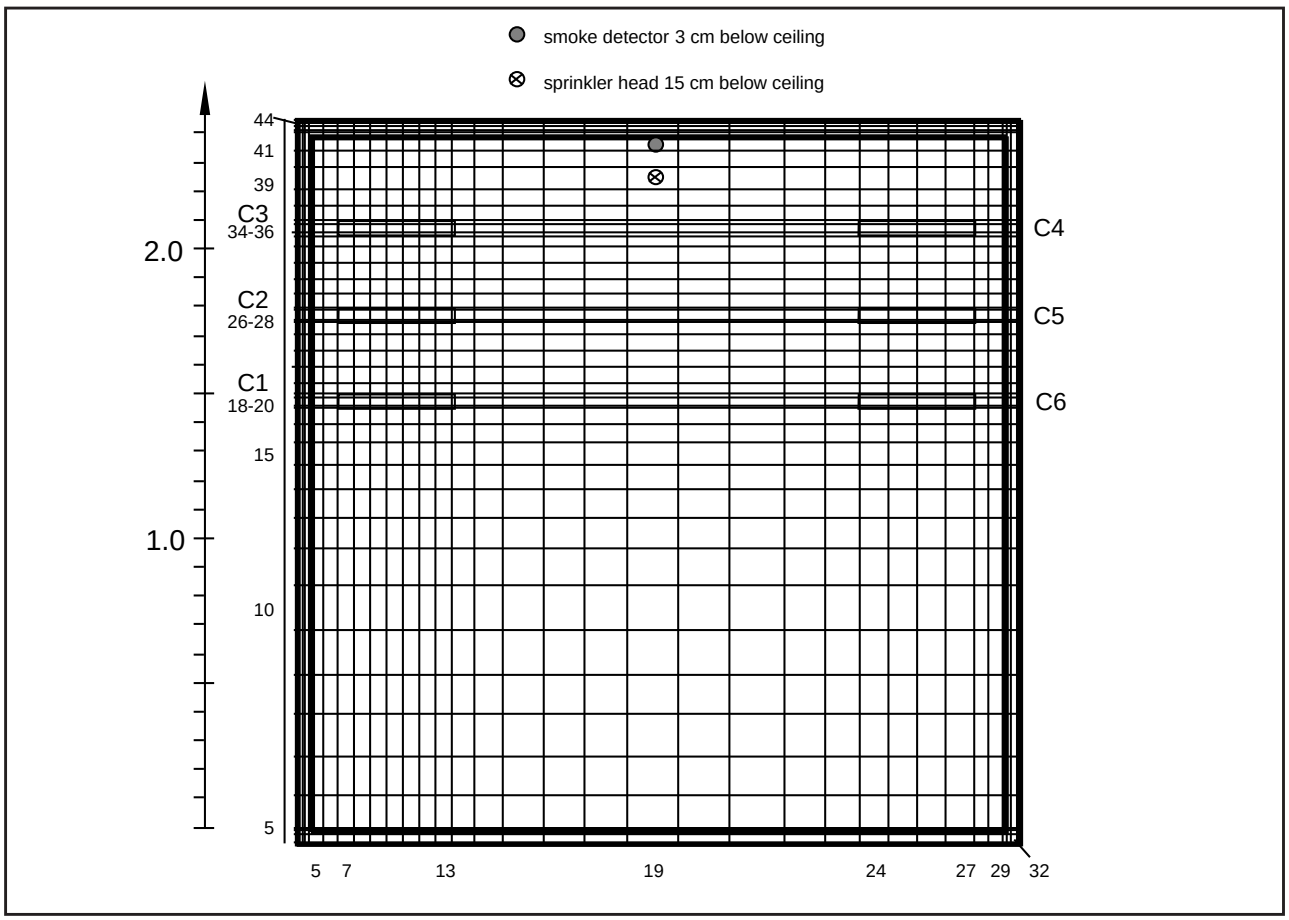

Figure 2. *Cross section of the tunnel. Cable trays C1-C6 are modelled in the simulation. The computational grid is presented here in a simplified form to give an impression of the density of the grid. In the actual grid the cells in the middle part are distributed more evenly in the vertical direction (not shown in this picture).*

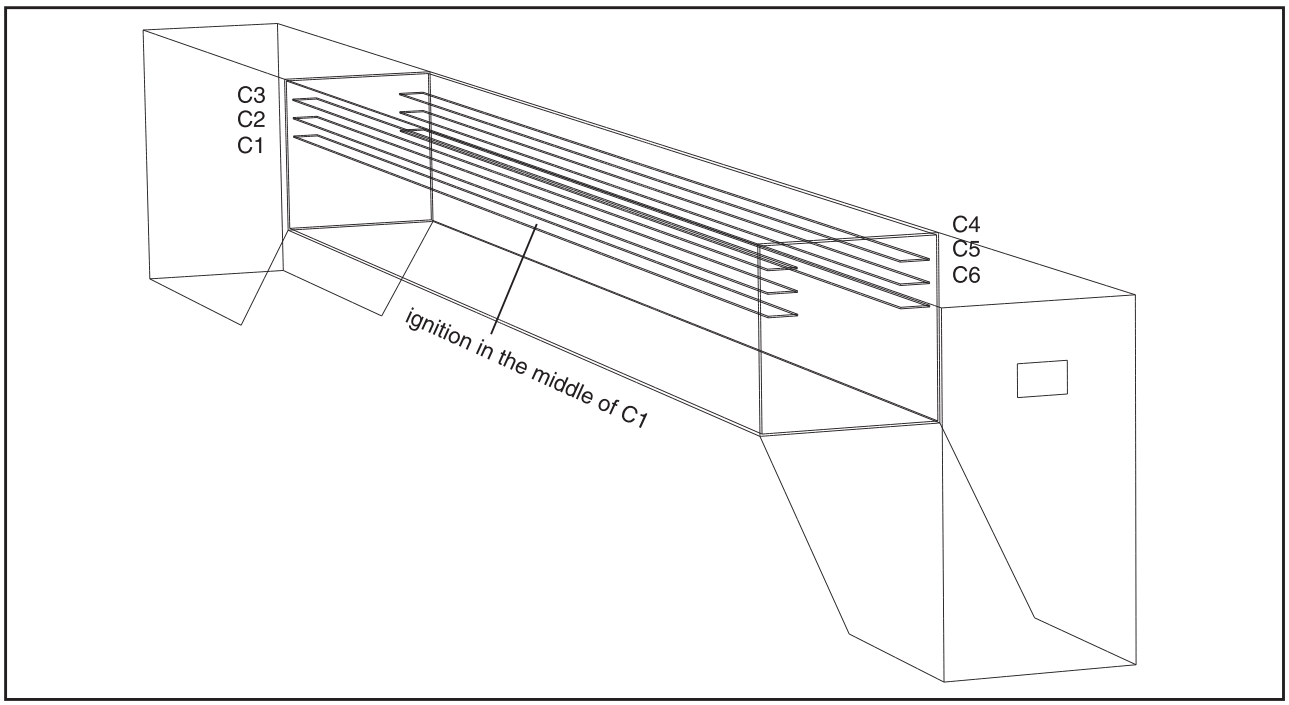

Figure 3. *Computational domain used in the simulation. Cable trays C1–C6 are modelled in the middle part of the tunnel. The fire starts from tray C1. The hole to the outer atmosphere is shown in the right end of the tunnel.*

order-upwind discretisation has been used for all the field variables. Time step over the whole time span is 1 second.

The connection outside the tunnel is defined through a hole in the other end of the tunnel (see Figure 3) where a constant total pressure has been defined. The real tunnels of interest may have different types of boundary conditions and this is considered as a compromise of different configurations. It is remarked that for example a tunnel ventilation would affect very much to the flow, smoke and temperature fields.

The smoke detectors are located on the center axis of the tunnel 3 cm below the ceiling. The planned distance between detectors is 6 m. In order to cover two cases with the fire source either abeam a detector or between two detectors, sample points are located 3 m from each other. Sample point locations are shown schematically in Figure 4.

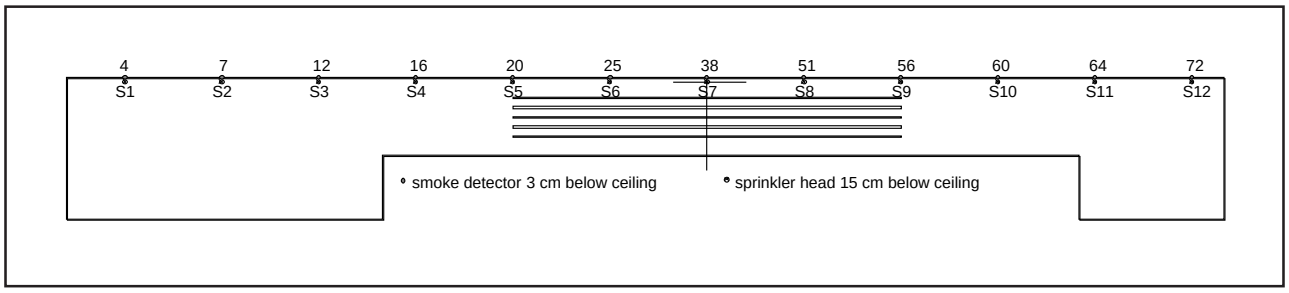

Figure 4. *Smoke detector sample locations on the ceiling of the tunnel. The numbers refer to the computational cell index in the tunnel axis direction. Smoke detectors S1–S12 are located at the centerline of the tunnel 3 cm below the ceiling. Sprinkler heads are in the same places 15 cm below the ceiling. The distance between adjacent locations is 3 m.*

3 SMOKE AND FIRE SPREAD MODELS

3.1 Smouldering fire

Smouldering phase of the fire is described with a constant heat and smoke source on cable tray C1. The heat release rate was chosen as an input to the simulation.

In this case no initial temperature stratification is assumed in the atmosphere. In a stratified case even a mild temperature difference might affect the flow field as stated in [7] where a mild stratification limited the plume over a heat source of 50 W. The plume penetrated though the upper layer when the source was 200 W. The 50 W heat release rate is chosen for the smouldering phase. This rate is the power released to the gas phase.

The heat release rate $\dot{q}$ of a smouldering fire is related to the fuel release rate $\dot{m}_{fu}$ by

$$\dot{q} = \chi \dot{m}_{fu} H_{fu} \tag{1}$$

where χ is the efficiency factor and H_{fu} the heat of combustion of the burning material. According to the experiences in [3] the efficiency factor is considered to be 0.1. The fuel release rate calculated from (1) is used as a basis for the smoke release rate.

The source for smoke mass fraction is estimated by using the smoke conversion factor ε from literature. SFPE Handbook [8] gives a range 0.03…0.12 for the smoke conversion factor for smouldering PVC fire. The value 0.1 is chosen for the simulation. The smoke mass source $\dot{m}_{smoke}$ is

$$\dot{m}_{smoke} = \varepsilon \dot{m}_{fu} \tag{2}$$

3.2 Smoke density

The smoke mass fraction is solved from a field equation as a conserved scalar. The local absorption coefficient K_{smoke} is estimated from the smoke concentration c_{smoke} with equation

$$K_{smoke} = K_m \; c_{smoke} \tag{3}$$

where the coefficient K_m has a value 4 400 m²/kg in a pyrolysing fire and 7 600 m²/kg in a flaming fire [8]. The optical density m (dB/m) is correlated with the absorption coefficient with equation [3]

$$m_{smoke} = 4.343 \; K_{smoke} \tag{4}$$

3.3 Smoke detection

The smoke detection time vs. smoke density is found from the detector experiments [4], [5]. The earliest and latest detection times are used to define a time frame where detection takes place. In some experiments, there were detectors that never gave an alarm during the experiment.

In the experiments, the detection time of different detectors for a smouldering PVC fire varied between 400–780 s [4]. The corresponding optical density of smoke near the detectors was in the range 0.01–0.3 dB/m [5]. This is used as a criterion for smoke detection in the simulation.

The maximum optical density of smoke in this experiment was about 0.3 dB/m. The range of critical smoke density is very large. This can result from differences in the detectors themselves. Also it is possible that the smoke densities were not equal at different detectors. The reference measurement was conducted at the symmetry axis of the experimental setup [4]. The detectors were located on an arch 3 m from the plume. The distance to the location of the optical density instrument was 0.275…1.5 m.

The often used criterion for smoke detection is temperature rise which correlates with smoke

density. Commonly, a temperature rise of 13°C is a criterion for detection [9], although other values, like 20°C, have been used as well. For new advanced detectors it is suggested that 4–5°C would be a proper value [9]. In flaming combustion this method may be an appropriate approximation, but in smouldering cases correlating the temperature rise to detection leads to great uncertainty. In a slow smouldering fire the heat transfer from plume is relatively high. Walls and other structures absorb the heat whereas the smoke concentration is not affected as much. It is remarked in [9] that when using temperature rise as an indication of smoke detection the walls should be considered as adiabatic.

3.4 Propagation model for cables

The fire spread model for horizontal cable trays is based on the work presented in [1]. The model includes criteria for ignition of a new tray, propagation of the flame front across the ignited tray and heat release rate (or rate of pyrolyzed fuel release) from the ignited surface.

The model relies on experimental data from cone calorimeter tests. Due to the limited experimental information the modified data set for MMO-A type cable is used. The set is the same as used in [1]. There are new cone calorimeter experiments underway, but the results are not yet available.

3.5 Sprinkler head response

Sprinkler head response can be calculated from the gas temperature history *T(t)*, the sprinkler head response time index (RTI) and the local gas velocity *u(t)*. The formula

$$\frac{dT_e(t)}{dt} = \frac{\sqrt{u(t)}}{RTI}\left(T_{gas}(t) - T_e(t)\right) \tag{5}$$

is used [1]. RTI = 80 $(m/s)^{1/2}$ is used for a fast sprinkler head and RTI = 300 $(m/s)^{1/2}$ for a slow sprinkler head. The critical value for the temperature of the sprinkler head, T_e, is 68°C.

4 SIMULATION

4.1 Smouldering phase and smoke detection

The case has been simulated as a smouldering fire for the first 11 minutes. After that it is assumed that flaming phase starts.

In the smouldering case the fire source is concentrated to a single cell in the middle of cable tray C1. The source is defined as a constant heat and smoke source.

At the beginning the atmosphere is at rest. The flow field develops very slowly due to the low heat release rate (50 W). Heat and smoke rises up on both sides of the cable tray. The smoke density calculated from smoke concentration is presented at detector locations in Figures 5 and 6. The distance between two adjacent detectors is 6 m. In this simulation the distance between follow-up points is 3 m. Thus we can cover both the case when the fire source is between detectors and abeam a detector.

The smoke density rises very steeply in the first phase. This is mainly due to the implementation of the source term which is defined as a step function from zero to the nominal value. In reality, the source grows under some time span and the first 'overshoot' should be smaller.

The fire alarm is given when one detector gives a signal. In some installations when two detectors give a signal the sprinkler system is activated. The detection range is 0.01…0.3 dB/m. Even at the higher limit it is possible that detection takes place in less than one minute after smoke production starts (Figures 5 and 6).

If the fire source is between the detectors, the fire alarm takes place after one minute from the start of smoke production. From Figures 5 and 6 it can be seen that the flow field is rather symmetrical at this stage. When the flow field is already fully developed the local smoke concentration becomes lower (when a constant smoke source is assumed).

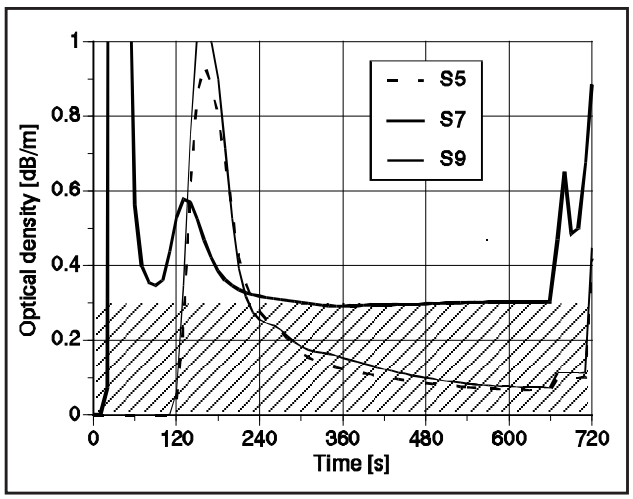

Figure 5. *Optical smoke density at detector locations when the fire source is abeam detector S7. Detectors S5 and S9 are located 6 m from S7 on opposite sides. The detection range (0.01–0.3 dB/m) is shown with a pattern.*

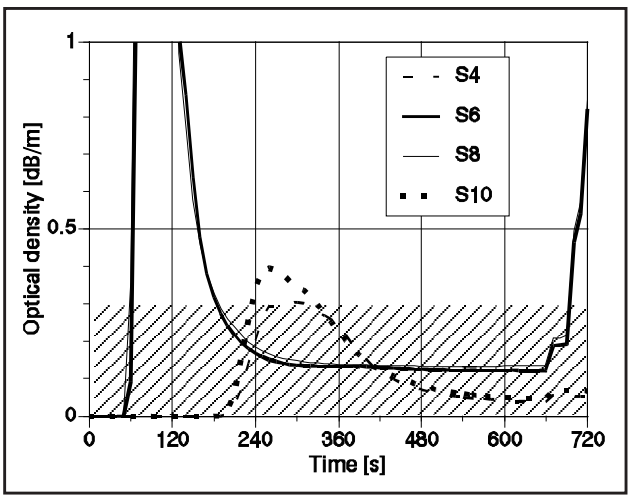

Figure 6. *Optical smoke density at detector locations S4–S10. The fire source is located between detectors S6 and S8. The detection range (0.01–0.3 dB/m) is shown with a pattern.*

The iso-surface of smoke concentration is shown in Figure 7. The flow spreads across the tunnel ceiling evenly to all directions at this stage. The smoke layer is very thin and velocity and concentration gradients are high.

The temperature values have not risen very much during the smouldering phase. In Figure 8 the temperature field is presented in the cross section of the smoke source. Near the smoke detectors in the symmetry axis of the tunnel the temperature rise is only about 1°C.

Velocity near the smoke detectors is in the

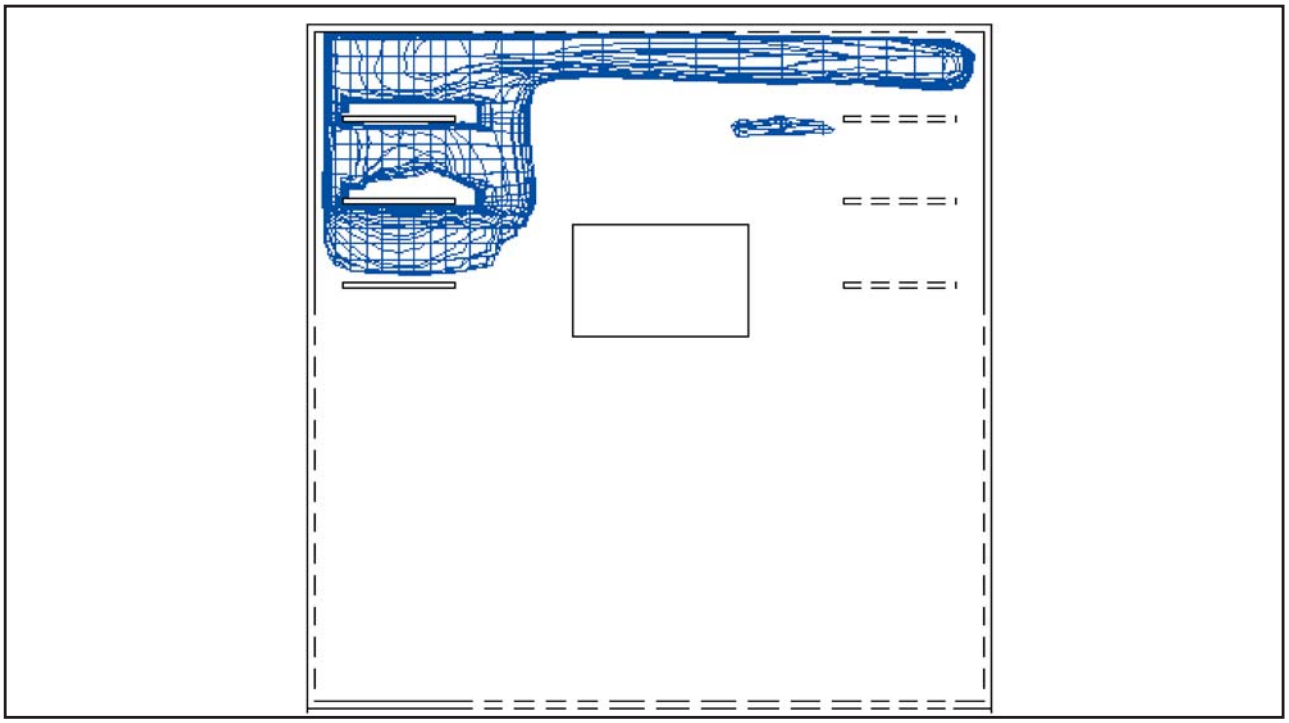

Figure 7. *Iso-surface of smoke concentration in the middle of the tunnel. Smoke mass fraction is* $7 \cdot 10^{-6}$ *at 600 s from the start of the smoke production.*

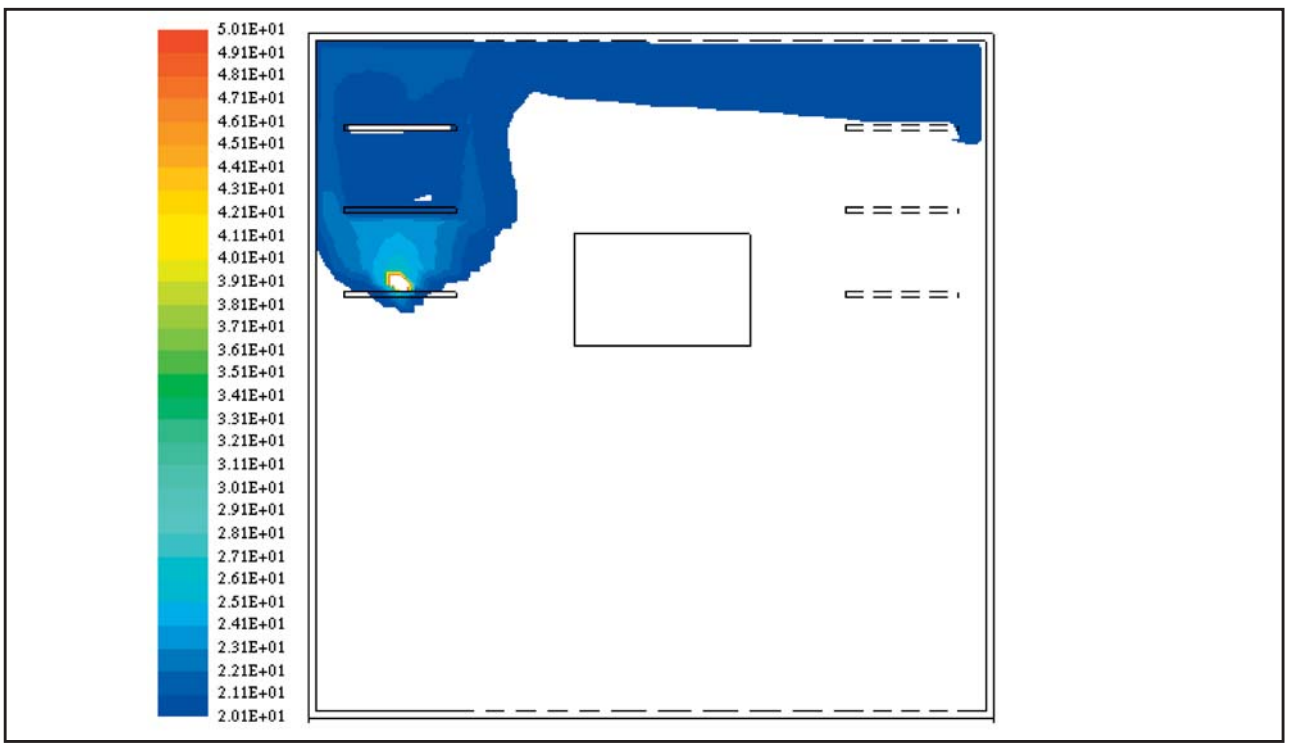

Figure 8. *Temperature field [°C] in the plane of smoke source at 600 s after the start of smoke production. The range in the whole domain is 19.6–84.4 °C. Temperature rise near the smoke detectors is about 1 °C.*

range of 0.01–0.05 m/s in the tunnel axis direction.

The dimensions of the plume are rather small in the smouldering case and the computational grid has been designed mainly for flaming fire conditions in which heat output and plume dimensions are much larger. Thus the smoke concentration calculations may have been affected by numerical accuracy problems due to the small heat output from a smouldering fire source. Numerical diffusion leads to lower temperature, lower species and smoke concentration and milder gradients of all field values. Thus for the numerical reasons the simulated detection time may be later than would appear in reality. However, it is believed that the uncertainty in defining the heat and smoke source in a smouldering fire has much larger effect to the field values than the effect of numerical accuracy.

4.2 Flaming phase

This simulation gives no clue to the smouldering time or transition from smouldering to flaming phase. The smouldering phase could be continued further, but the conditions are quite stable and further simulation could not bring forth new information. Therefore, the beginning of the flaming phase of the fire is given as an input.

At 11 minutes it was defined that the lowest tray C1 is ignited and fire continues as a flaming one. After this, the flame front and fuel release rate are modelled according to the spread model [1]. The rate of heat release is presented in Figure 9 from ignition of tray C1 to 40 minutes. The present criterion for next object ignition does not predict the ignition properly. Thus the next tray C2 is ignited 'manually' in the simulation after 24 minutes. The ignition of tray C2 is justified by the corresponding temperature and rate of heat release conditions in a full scale experiment [2], which has been simulated earlier [1]. Cable tray C3 was ignited manually as well after 31 minutes. The ignition times of the cable trays are given in Table I.

Table I. *Ignition time of cable trays.*

Tray	Ignition time	Ignition type
C1	11 min	boundary cond.
C2	24 min	boundary cond.
C3	31 min	boundary cond.
C4	45.7 min	by radiation
C5	45.9 min	by radiation
C6	46.6 min	by radiation

Temperature field at the ignition cross section is presented in Figure 10 and in the plane of the cable trays in Figure 11 at times 24 minutes, 30

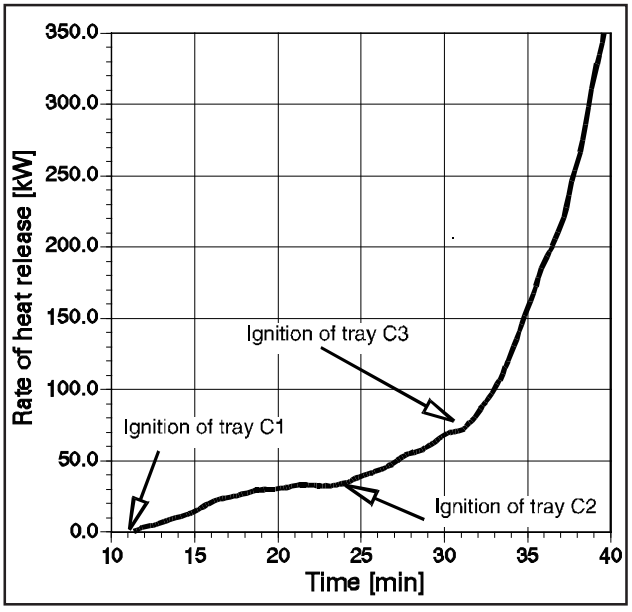

Figure 9. *Rate of heat release as a function of time after tray C1 has been ignited. Tray C2 is ignited 'manually' at 24 minutes and Tray C3 at 31 minutes.*

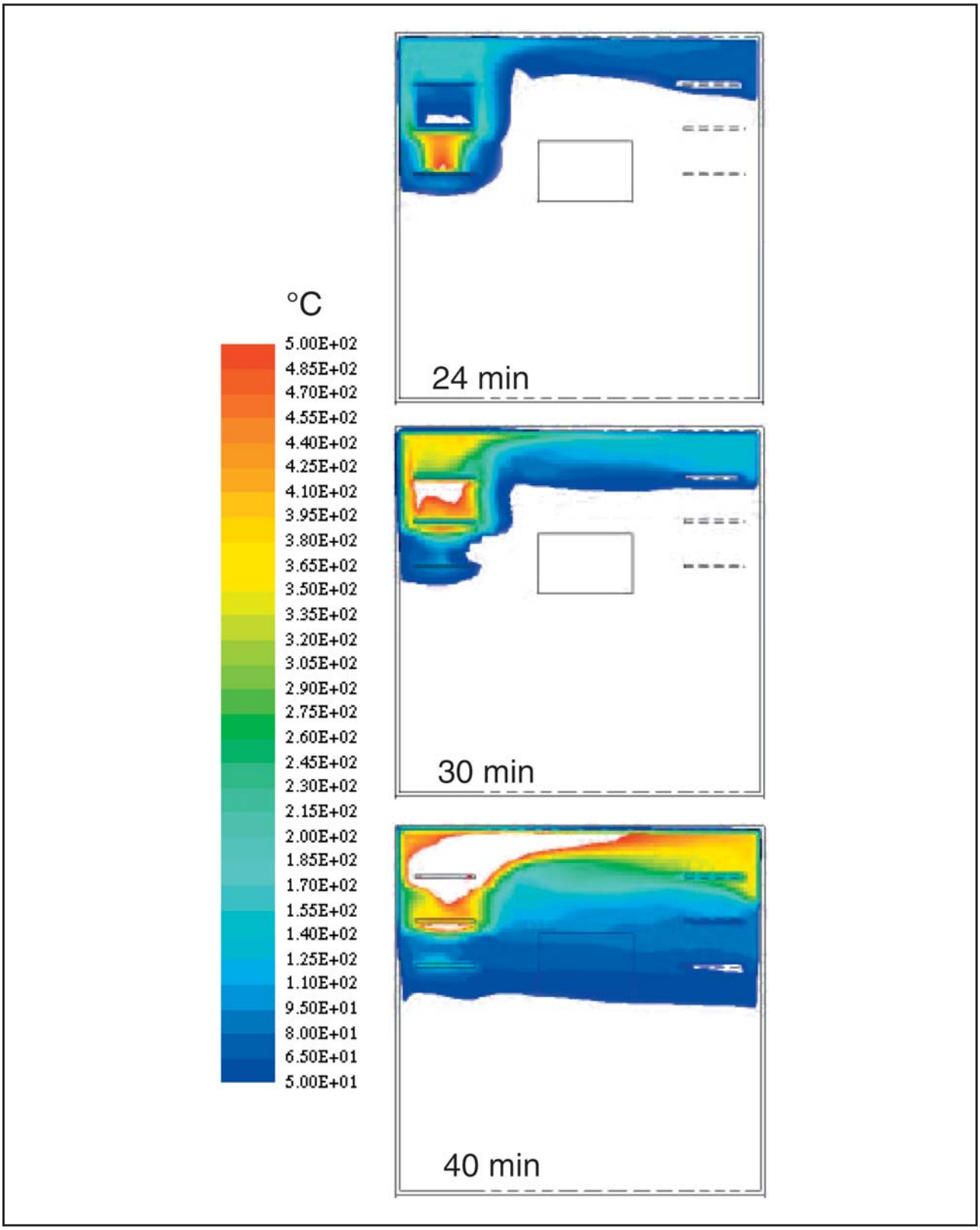

Figure 10. *Temperature field at the cross section where ignition takes place. a) At 24 minutes the temperature range in the whole field is 20–522 °C and the range in the plane is the same. b) At 30 minutes the temperature range in the whole field is 20–772 °C and in the plane 20–603 °C. c) At 40 minutes the temperature range in the whole field is 20–1315 °C and in the plane 20–1150 °C.*

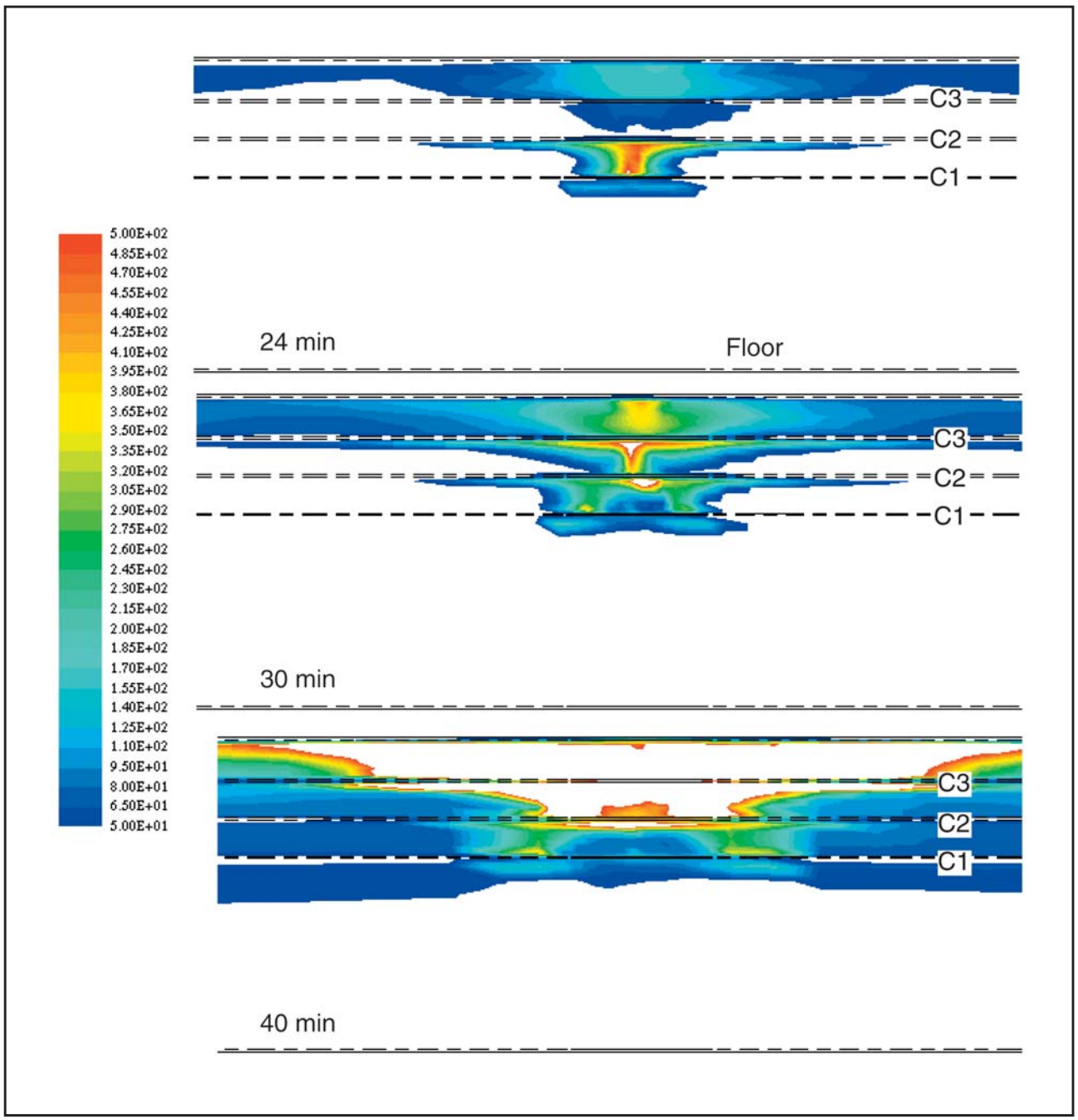

Figure 11. *Temperature field in the plane of cable trays C1–C3. a) At 24 minutes the temperature range in the plane is 20–522 °C, b) at 30 minutes the range is 20–772 °C and c) at 40 minutes 20–1270 °C. The corresponding rate of heat release is 34 kW, 69 kW and 390 kW in each case.*

minutes and 40 minutes. At these three moments the cable trays C1, C1–C2 and C1–C3 were burning and the heat release rate is 34 kW, 69 kW and about 390 kW respectively.

Temperature iso-surface under the tunnel ceiling is presented in Figure 12. The main flow is inclined about 45° from the tunnel axis. This suggests that under certain conditions it may not always be favorable to have a detector or sprinkler head just above the fire source in a tunnel fire. However, at a later stage when flame front proceeds further, the flow field changes.

The smoke concentration at 24–40 minutes is presented in Figure 13. The smoke proceeds to the ends of the tunnel and the atmosphere stays well staggered.

The rate of reaction is presented in Figures 14 and 15 at the original plane of ignition and at the plane of the cable trays. The area represents the 'flame', although the visible flame differs from the volume in which the chemical reactions take place. The local reaction rate depends on the local values of fuel and oxygen concentrations and turbulence time scale.

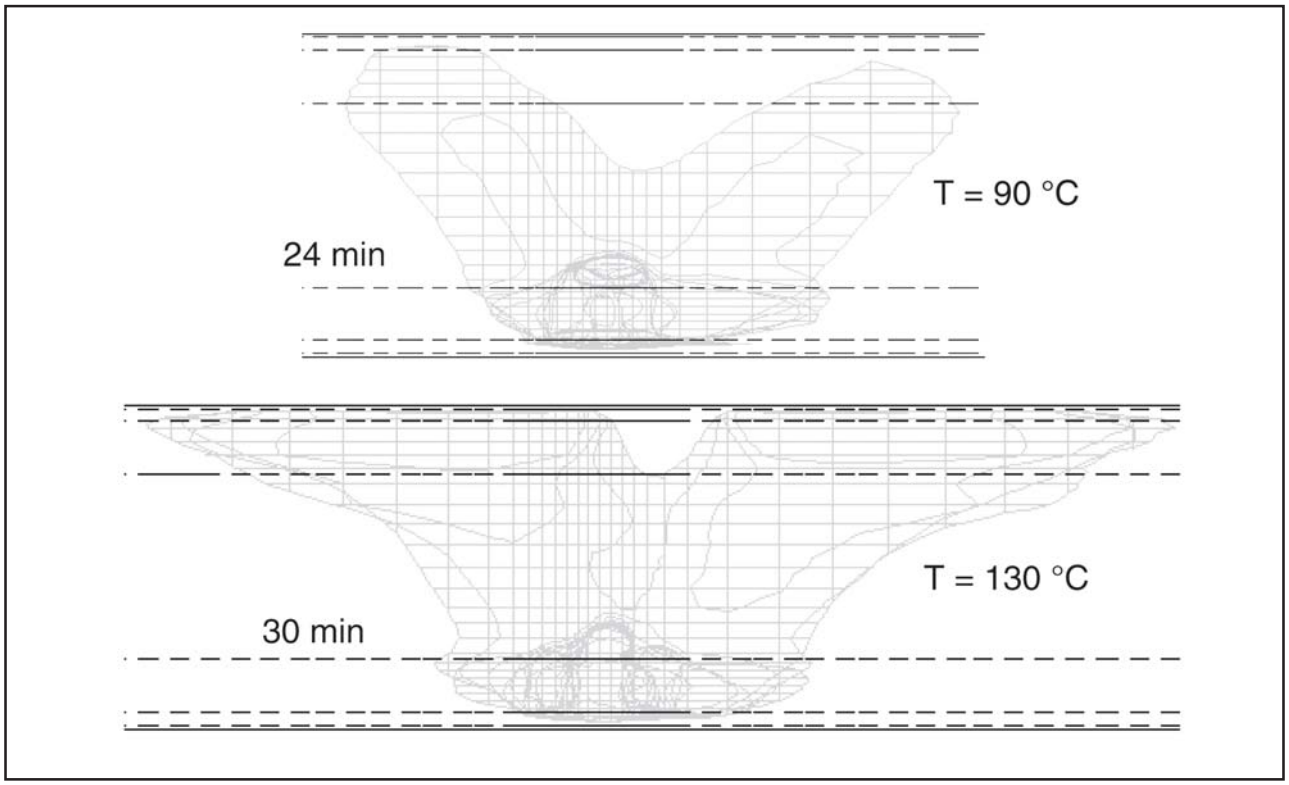

Figure 12. *Temperature iso-surface seen from top. The main flow under the ceiling is inclined about 45 °from the tunnel axis.*

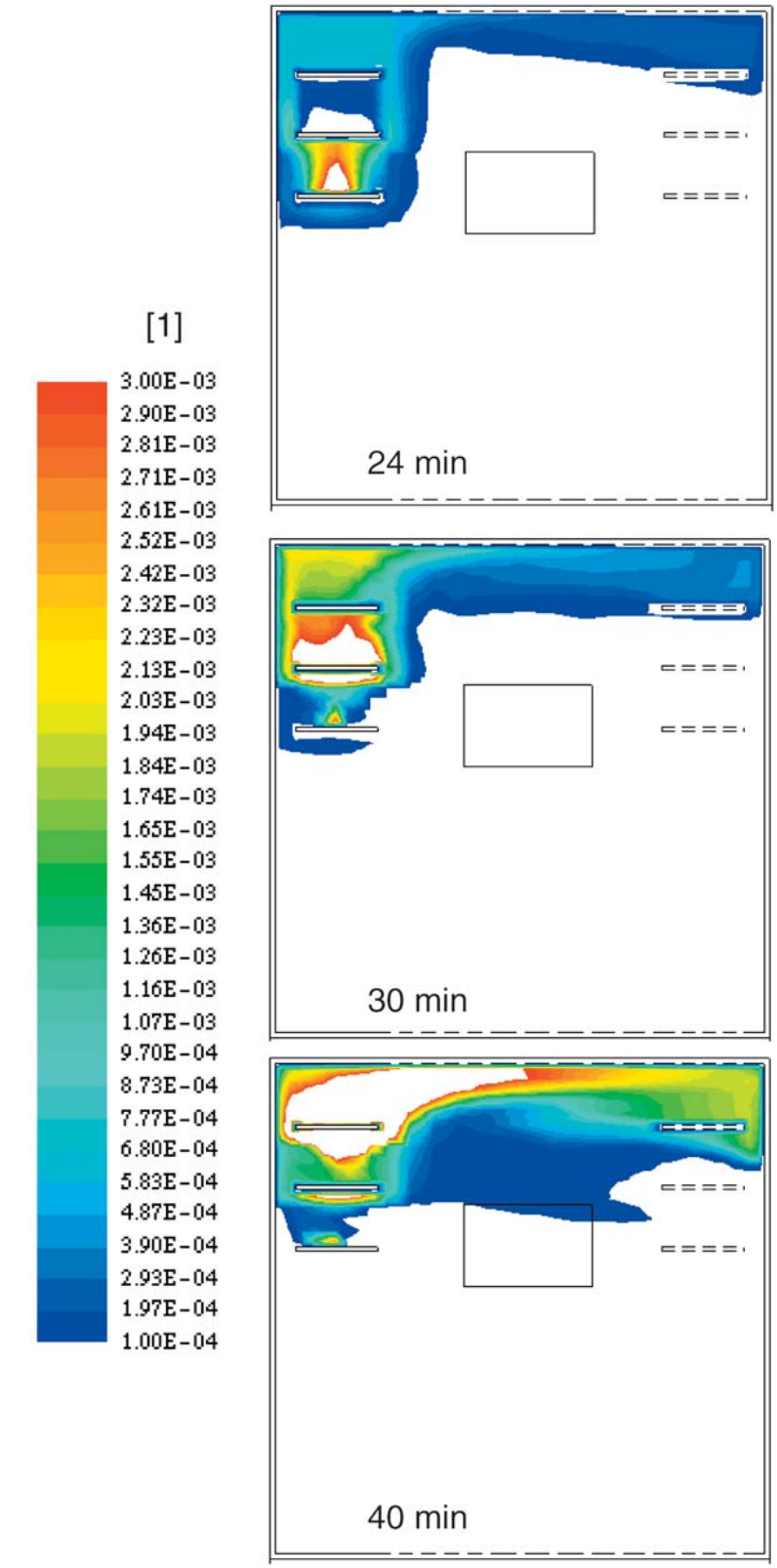

Figure 13. *Mass fraction of smoke at the plane of the fire source. The range of the mass fraction is a) 0–5.9·10^{-3} at 24 minutes, b) 0–9.6·10^{-3} at 30 minutes and c) 0–3.3·10^{-2} at 40 minutes.*

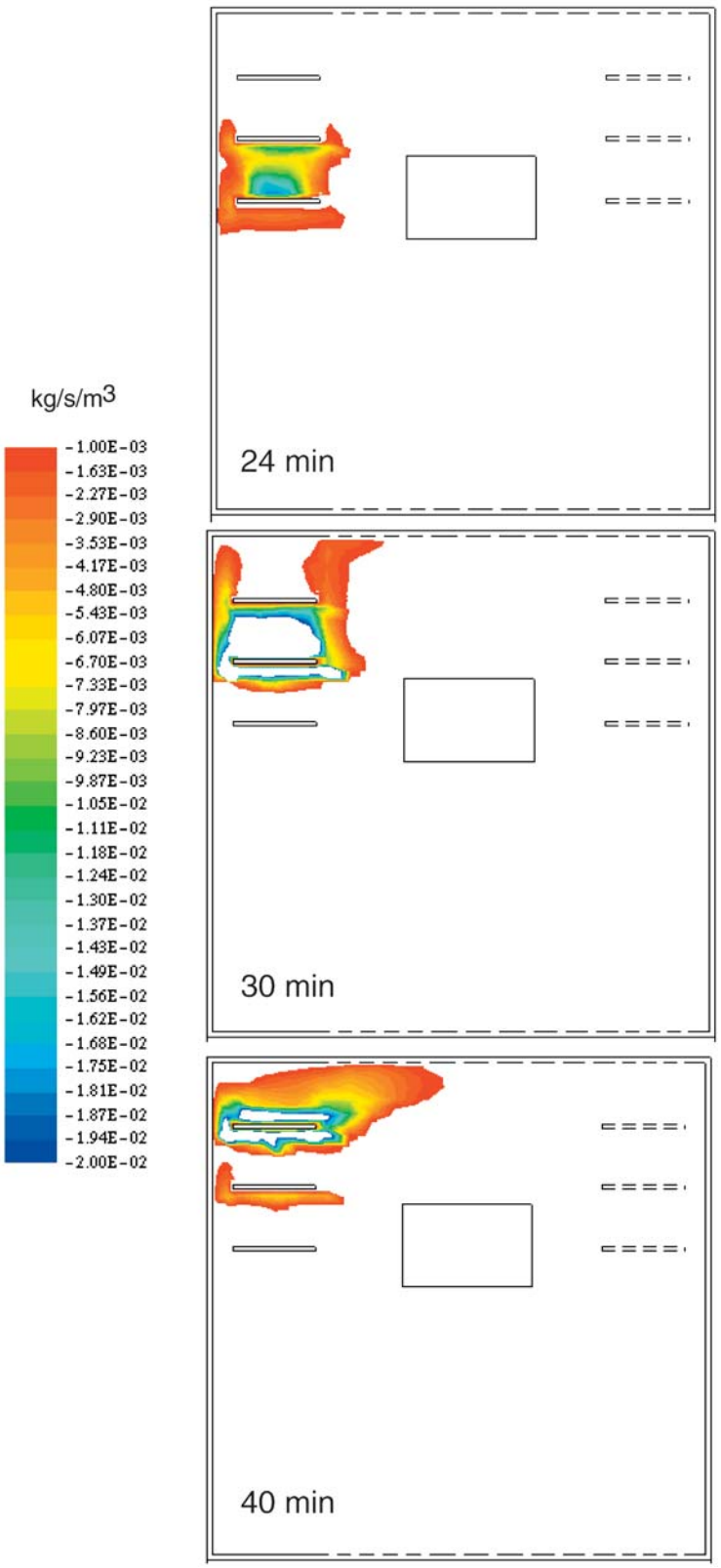

Figure 14. *Size of the reactive area at time 24–40 minutes seen at the ignition plane. The maximum fuel consumption values are –3.04·10^{-2} kg/m^{3}s, –1.27·10^{-1} kg/m^{3}s and –1.17·10^{-1} kg/m^{3}s at the different time steps, respectively.*

4.3 Heat flux at the opposite wall cables

The incident heat flux on the cable trays at the opposite wall of the tunnel is shown in Figure 16 at different time steps. In the model the incident heat flux has been used as a criterion for ignition. It is recognised, however, that the criterion is insufficient in order to predict ignition properly. Ignition depends also on the local concentrations of fuel and oxygen, the local temperature and temperature history of the solid material. Nevertheless, the incident heat flux gives a rough estimate of the conditions on the opposite cable trays.

The local temperature in the hot layer does not rise as quickly as in the experiment [2] because the volume of the tunnel is much larger than the volume of the experimental room.

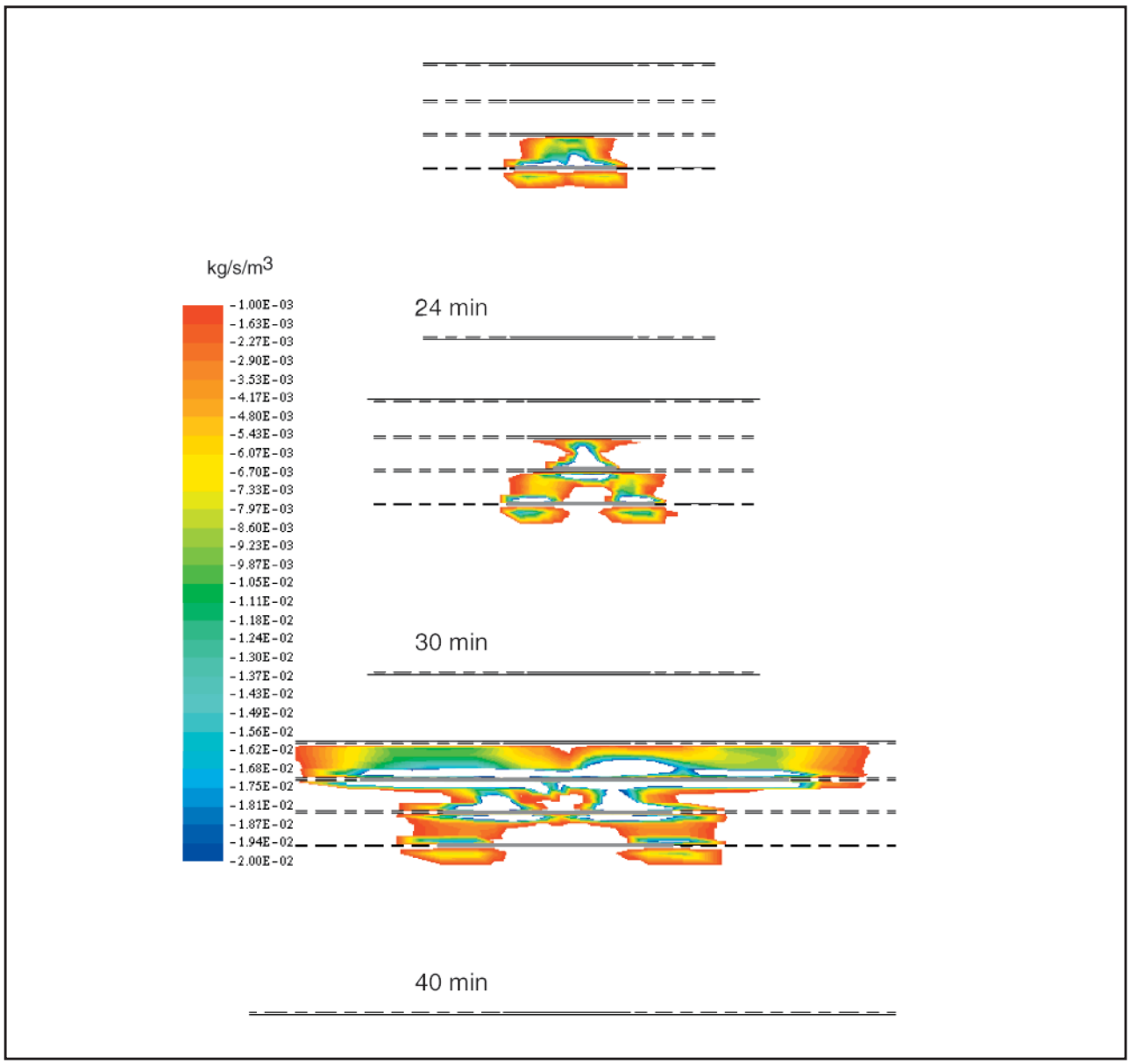

Figure 15. *Size of the reactive domain at time 24–40 minutes seen at the plane of the trays. The maximum fuel consumption values are $-3.04 \cdot 10^{-2}$ kg/m^{3}s, $-1.27 \cdot 10^{-1}$ kg/m^{3}s and $-1.17 \cdot 10^{-1}$ kg/m^{3}s at the different time steps, respectively. The length of the burning area on the cable trays are show with a coloured stripe on the tray. The burning lengths are 0.86 m (C1) at 24 minutes, 1.27 m (C1) and 0.53 m (C2) at 30 minutes and 2.05 m (C1) 2.0 m (C2) and 3.75 m (C3) at 40 minutes.*

Table II. *Response time of sprinkler heads. Time is measured from the beginning of smouldering phase. For location of the sprinkler heads, see Figure 4. Sample points are located 3 m from each other.*

	Fast RTI 80 (m/s)^{½}	Slow RTI 300 (m/s)^{½}
S4	28.0	31.8
S5	25.7	29.8
S6	20.2	27.3
S7	**19.3 (–27)**	**26.7 (–36)**
S8	22.0	27.8
S9	24.8	29.0
S10	27.5	31.3

4.4 Sprinkler head response

In addition to the smoke detection, the sprinkler head response to the temperature and flow was estimated. In smouldering phase the sprinkler heads, which are sensitive to temperature rise, are practically not at all affected by the extremely small change of temperature in the smoke layer. In the flaming phase, the temperature rise is larger and the response of the sprinkler heads is estimated using the guidelines found in [1]. For the sprinkler head response time index (RTI), the value 80 $(m/s)^{1/2}$ is used for fast heads and 300 $(m/s)^{1/2}$ for slow heads in order to get an estimate for early and late activation.

The temperature rise and local velocity component in the tunnel axis direction are shown in Figures 17 and 18.

The estimated sprinkler response time is given in Table II, in which time is measured from the beginning of smouldering phase (which took 11 minutes). The location S7 is at the original ignition plane and the other locations 3 m to both directions (see Figure 4).

In Table II, a time span is given for the head S7. The local flow field develops so that in the source plane the local velocity near the sprinkler head is very low due to the countercurrent reflecting from the opposite wall (see Figure 19). If the ignition source is exactly abeam the sprinkler head, the heat transfer from the flow to the sprinkler head bulb is low due to the low local gas velocity. This leads to a later activation time

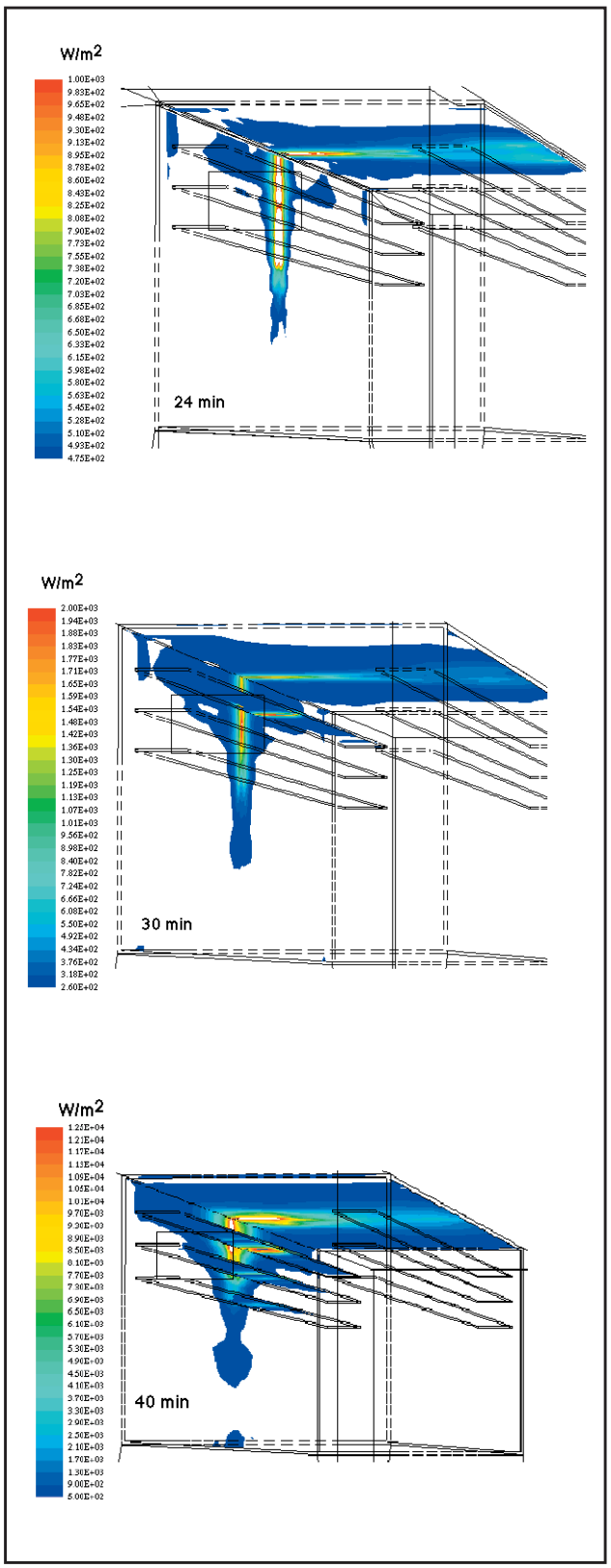

Figure 16. *Incident heat flux on the surfaces around the fire source at time 24 minutes, 30 minutes and 40 minutes. The maximum values on the cable trays are 3.5 kW/m² (C1), 4.9 kW/m² (C3) and 44.6 kW/m² (C3) at different time steps respectively.*

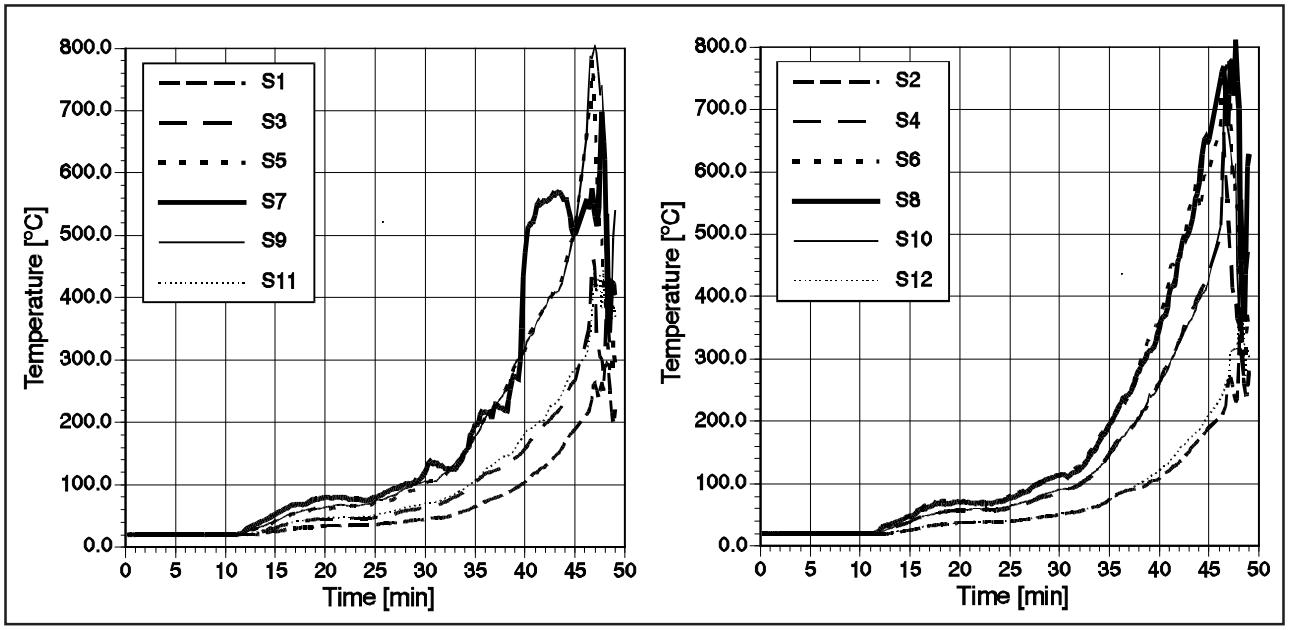

Figure 17. *Gas temperature at different sprinkler head locations as a function of time. For the location of the sprinkler heads, see Figure 4. The location S7 is on ignition plane. Values at S5–S8 appear to be rather identical for the first 40 minutes. Temperature field on the tunnel axis is symmetrical with respect to the ignition plane.*

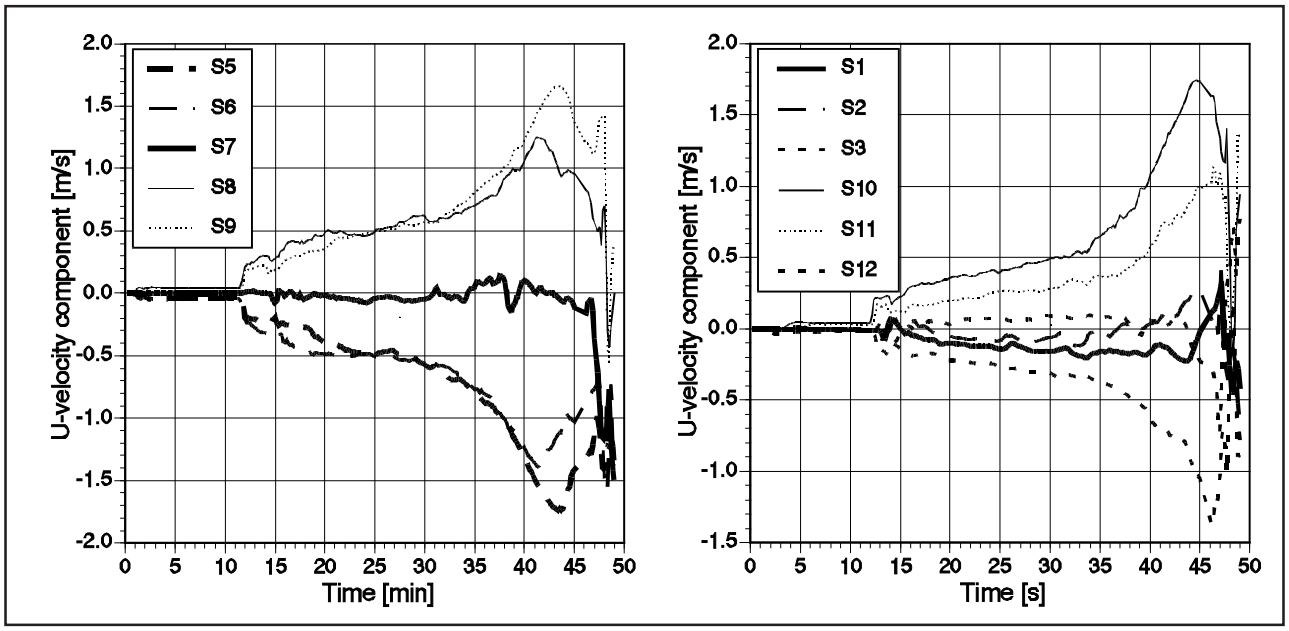

Figure 18. *Velocity component in the tunnel axis direction at different sprinkler head locations as a function of time. Flow field appears to be symmetrical with respect to the ignition plane near the sprinkler heads S5–S9. The field becomes more distorted near the tunnel ends due to different boundary conditions.*

which is shown in parentheses in Table II. However, the low velocity area is very narrow and it is possible that due to other disturbances this would not even appear in a practical case. For this reason the activation time for S7 is estimated by using the velocity at the next sprinkler heads.

From Figure 19 it can be seen that the velocity gradient is very steep below the ceiling. Same applies to the temperature gradient as well. Thus the activation time depends on the distance of the sprinkler head and ceiling.

In estimating response time of the later activating heads, the sprinkler influence to the fire and flow conditions has not been taken into account in any way. The activation of the sprinkler would change the flow and heat release rate development essentially. This would affect to the activation time of the rest of the sprinkler heads.

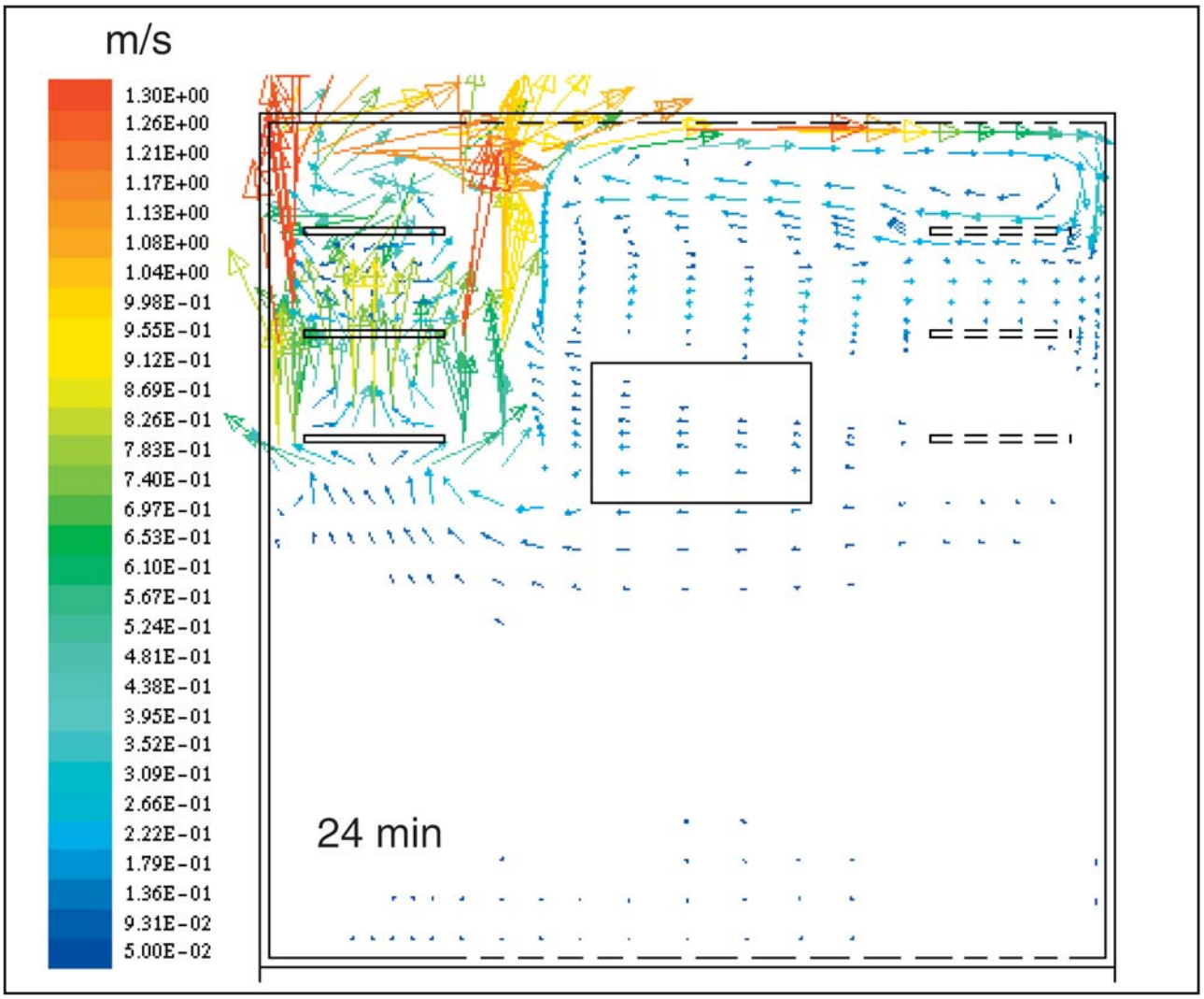

Figure 19. *Velocity field in the ignition plane at 24 minutes. Vector range 0.05–1.3 m/s is shown in the picture. Maximum value in the domain is 1.39 m/s.*

which is shown in parentheses in Table II. However, the low velocity area is very narrow and it is possible that due to other disturbances this would not even appear in a practical case. For this reason the activation time for S7 is estimated by using the velocity at the next sprinkler heads.

From Figure 19 it can be seen that the velocity gradient is very steep below the ceiling. Same applies to the temperature gradient as well. Thus the activation time depends on the distance of the sprinkler head and ceiling.

In estimating response time of the later activating heads, the sprinkler influence to the fire and flow conditions has not been taken into account in any way. The activation of the sprinkler would change the flow and heat release rate development essentially. This would affect to the activation time of the rest of the sprinkler heads.

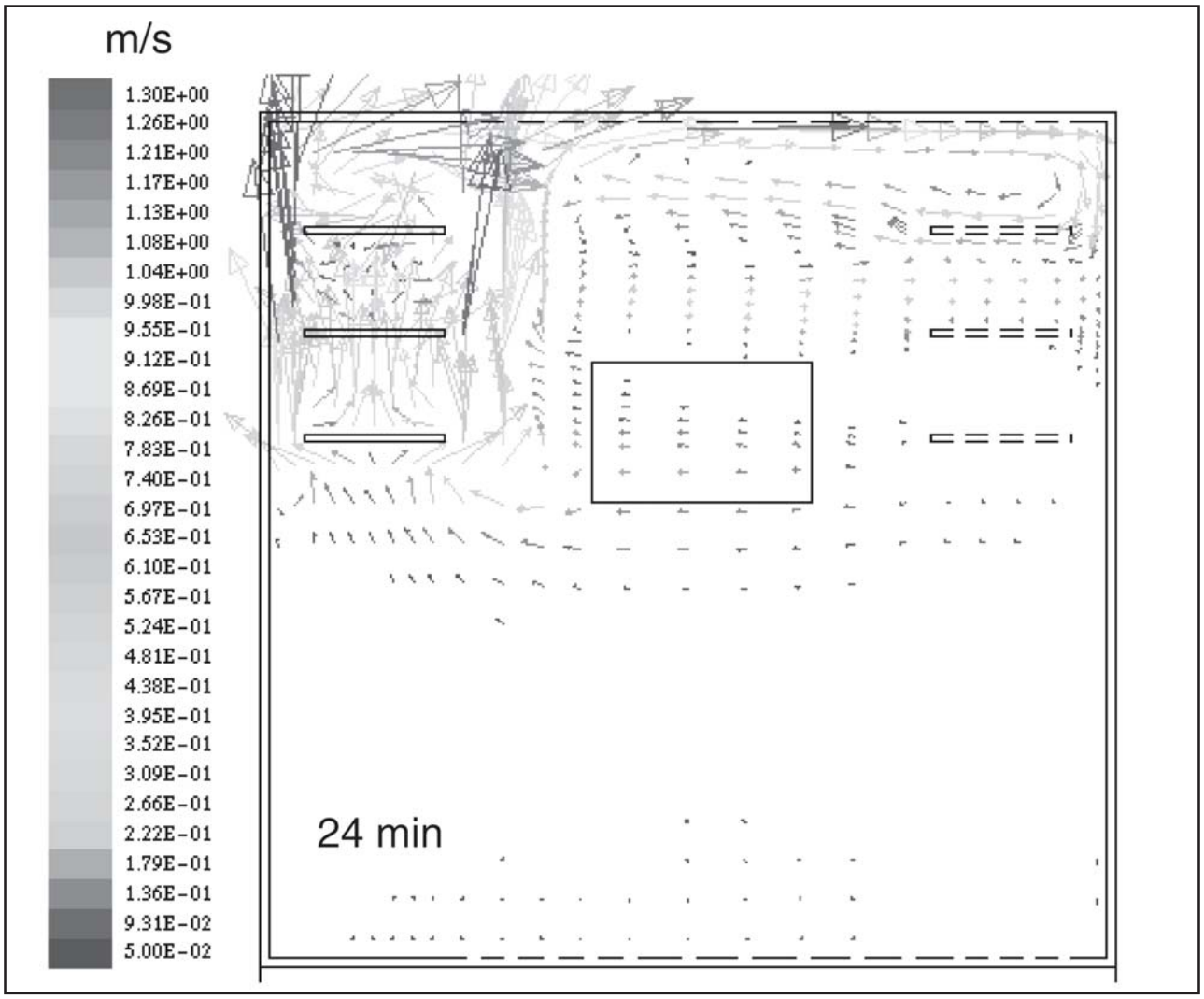

Figure 19. *Velocity field in the ignition plane at 24 minutes. Vector range 0.05–1.3 m/s is shown in the picture. Maximum value in the domain is 1.39 m/s.*

4.5 Conditions at the selected moments

After the smouldering process starts, the smoke spreads to the smoke detectors in 1–2 minutes depending on the distance between the source and the detector (under the conditions assumed here). This time interval can be affected by for example tunnel ventilation. In the simulation it is assumed that ventilation is not present. If ventilation is active it would affect especially to the smouldering phase where the source terms and thus buoyancy are weak.

In the smouldering phase, the only effect of the

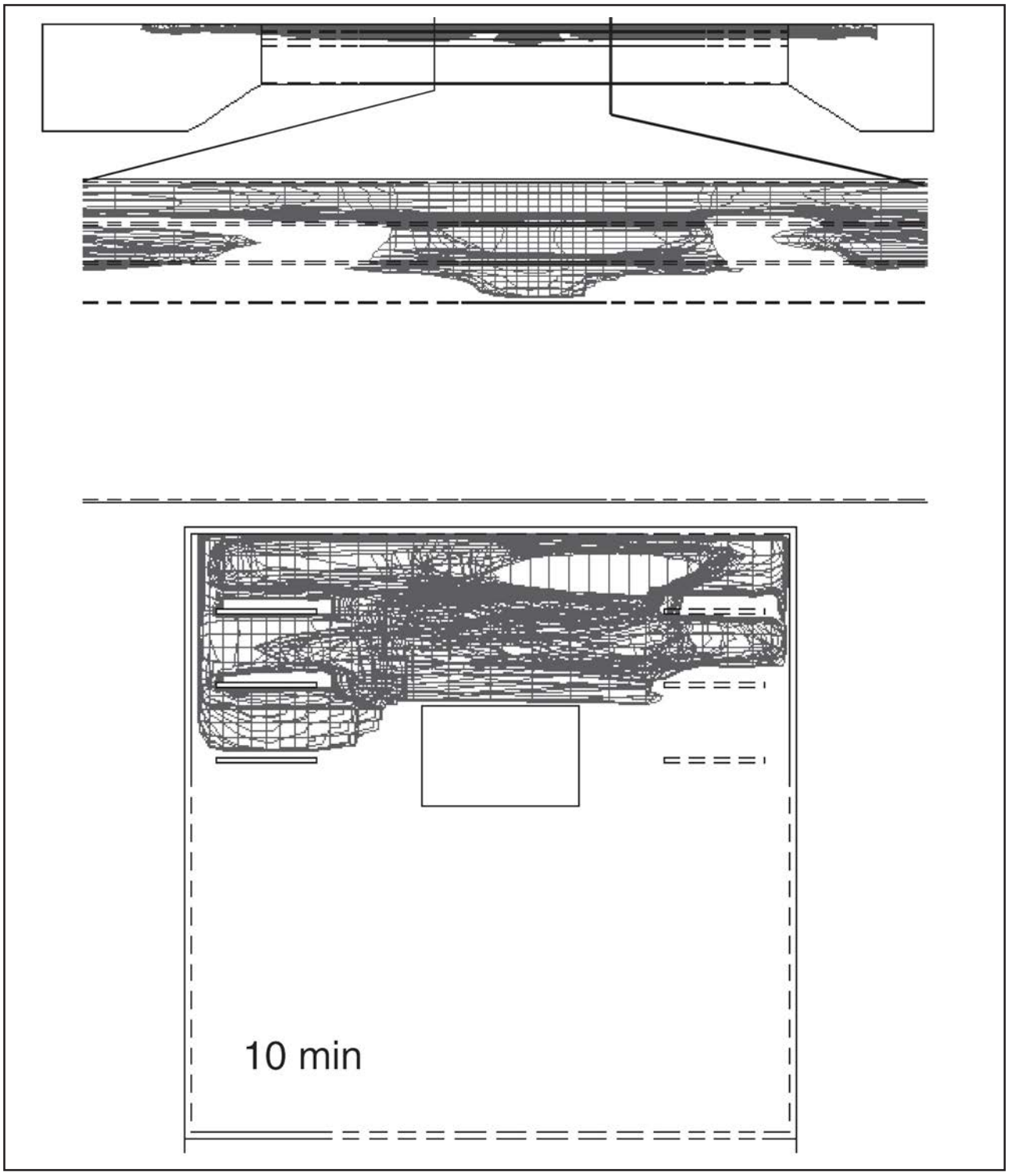

Figure 20. *Smoke mass fraction of $2 \cdot 10^{-6}$ at 10 minutes seen at the plane of the cable trays C1–C3 and from the end of the tunnel.*

fire is the smoke production and the local damage in the smouldering object itself. The temperature field is not affected very much, only about 1°C compared to the initial conditions. The smoke mass fraction at 10 minutes is presented in Figure 20.

In the flaming phase the first moment of interest is the time when the sprinkler heads are activated. With fast heads the activation time is about 20 minutes and with slow heads about 27 minutes. At this time the cable trays C1–C3 are damaged seriously and the interest is in the cable trays C4–C6. What are the conditions on the opposite wall trays? The temperature profile along the upper side of the cable tray C4 and below the ceiling are presented in Figure 21. The incident radiative heat flux to the upper surface of tray C4 is presented in Figure 22.

As it can be seen from Figure 21 a, the local temperature below the ceiling is not very high at 20 minutes or 27 minutes and can not emit such a radiative heat flux that would damage the cable insulation. As observed in Figure 21 b, the gas around the cables is not very hot. If the sprinklers, with the fast or slow heads, are able to extinguish the fire, the possibility of a short circuit of the cables on trays C4–C6 may remain small at this stage.

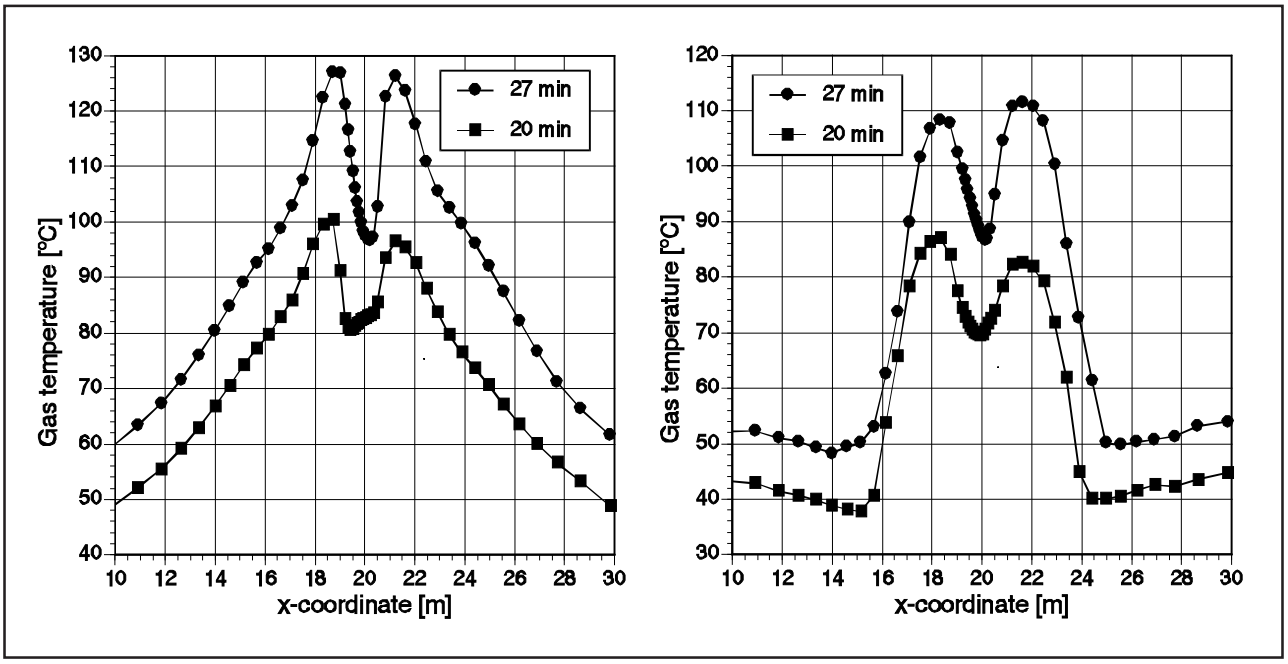

Figure 21. *The temperature profile a) below the ceiling and b) just above the cable tray C4 at 20 minutes and 27 minutes.*

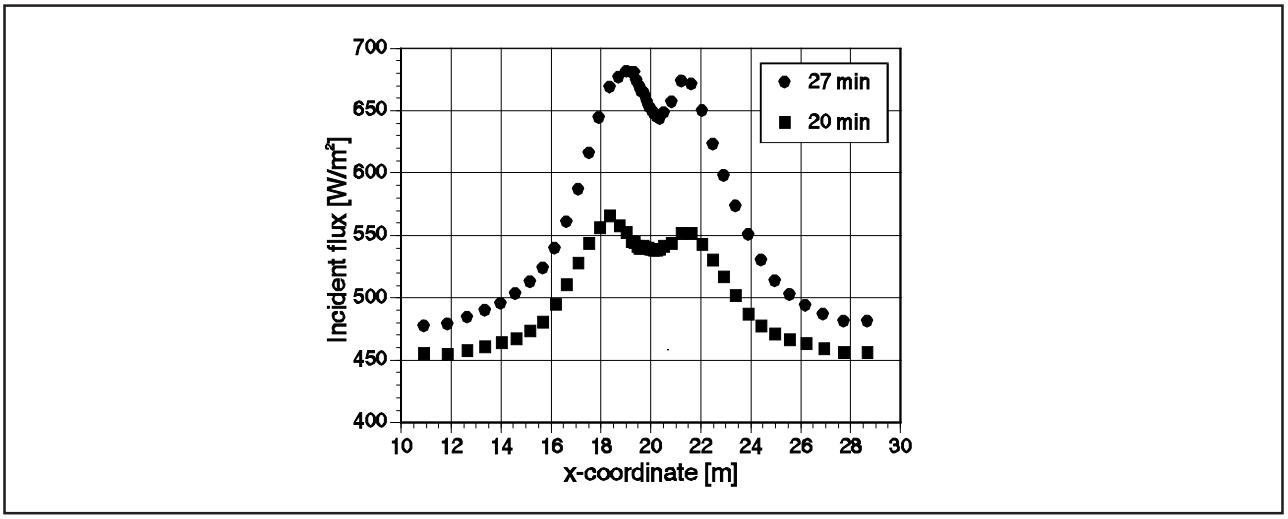

Figure 22. *The incident radiative heat flux on the cable tray C4 at 20 minutes and 27 minutes.*

The temperature profiles in vertical direction at selected locations are presented in Figures 23 and 24. In Figure 23 the profiles are at sample locations S6–S8 at the center axis of the tunnel. In Figure 24 the profiles are from the same axial locations but on the plane of the cable trays C4–C6. From the Figures it can be seen that the highest temperature near the upper surface of tray C4 is about 110°C at 27 minutes. The temperature gradient between the hot and cold layer is very steep. The temperature at the lower trays C5–C6 is essentially lower at this stage.

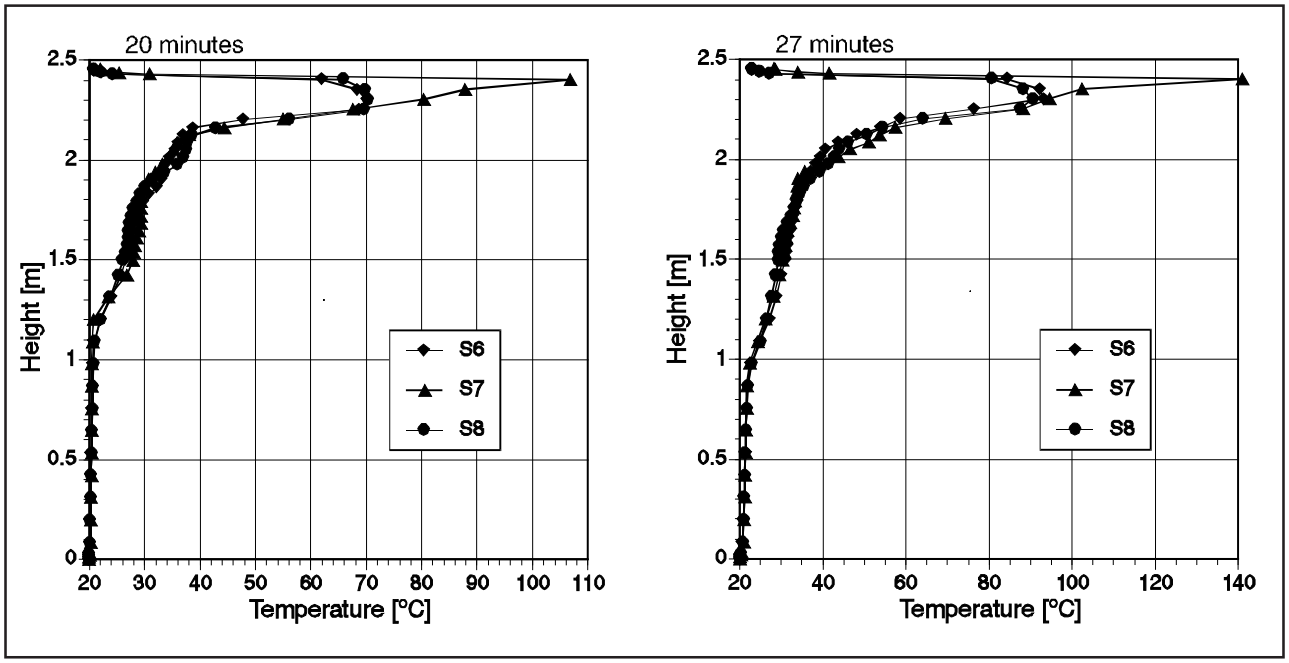

Figure 23. *Vertical temperature profiles at locations S6–S8 at 20 minutes and 27 minutes.*

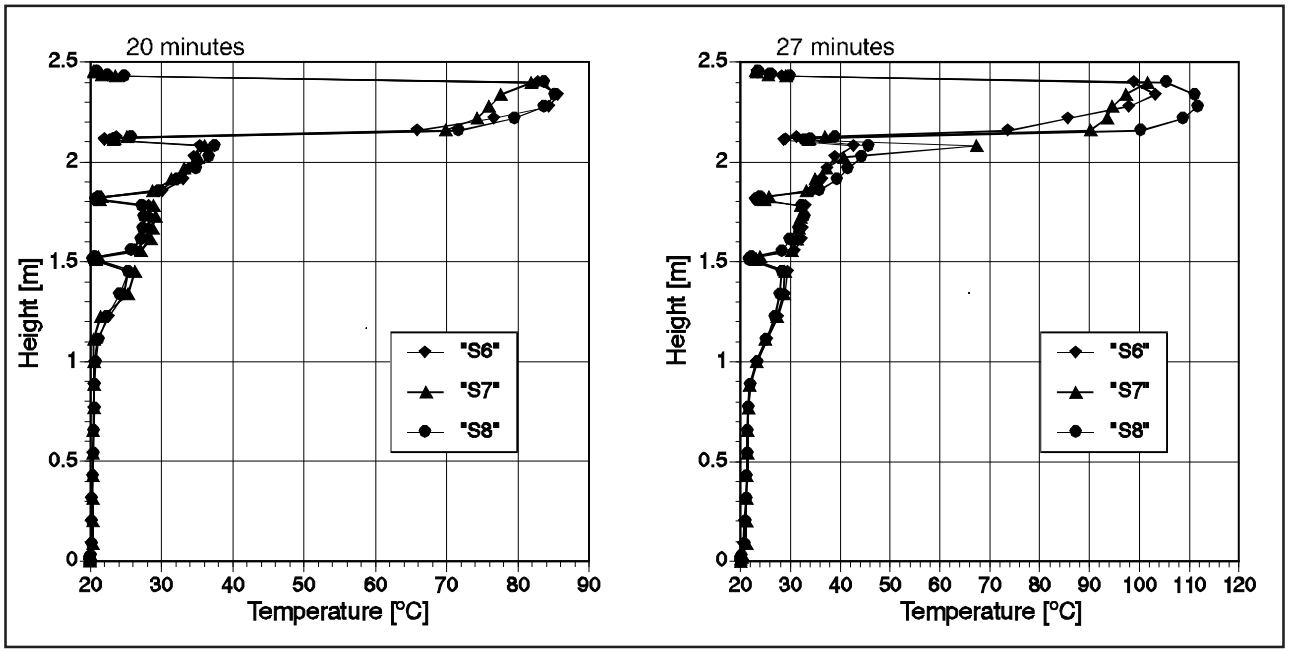

Figure 24. *Vertical temperature profiles at the axial locations S6–S8 but on the plane of the cable trays C4–C6 at 20 minutes and 27 minutes. The height of the cable trays are 1.5 m, 1.8 m and 2.1 m which can be seen in the temperature profiles.*

5 SUMMARY

A fire simulation of a full scale tunnel was performed by using the commercial code FLUENT as the simulation platform. Estimation was made for fire spread on the stacked cable trays, possibility of fire spread to the cable trays on the opposite wall of the tunnel, detection time of smoke detectors in the smouldering phase and response of sprinkler heads in the flaming phase.

According to the simulation, the temperature rise in the smouldering phase is minimal, only of the order 1°C. The estimates of optical density of smoke show that normal smoke detectors should give an alarm within 2–4 minutes from the beginning of the smouldering phase, depending on the distance to the detector (in this case it was assumed that the thermal source connected to the smoke source was 50 W).

The flow conditions at smoke detectors may be challenging, because the velocity magnitude is rather low at this phase. At 4 minutes the maximum velocity at the detectors is 0.12 m/s. Low gas velocity may cause delay to the detector response.

Fire spreads on the stacked cable trays in an expected way, although the ignition criterion seems to perform poorly when ignition of new objects is considered. The upper cable trays were forced to ignite by boundary condition definitions according to the experience found from a full scale experiment [2] and an earlier simulation [1]. After 30 minutes the hot layer in the room becomes so hot that it speeds up the fire spread and the rate of heat release of burning objects. Further, the hot layer ignites the cable trays on the opposite wall of the tunnel after 45 minutes.

Sprinkler heads are activated at 20–22 minutes near the fire source and at 24–28 minutes little further when fast sprinkler heads are used. The slow heads are activated between 26–32 minutes. The maximum temperature near the opposite wall cable tray C4 at 27 minutes is about 110°C which is not high enough to damage the insulation material in a short exposure time and if the sprinklers are able to extinguish the fire.

The simulation time of the 49 minute transient on a DEC AlphaServer 4100 computer is about 590 CPU hours when 1 s time steps are used. The computer time could be reduced if the parallel version of Fluent would be more efficient. However, in the used versions 4.4.8 and 4.5.2 the parallelisation seems to improve the code performance only marginally.

REFERENCES

1 Huhtanen R. Fire spread model for horizontal cable trays. Research report ENE21/11/98. VTT Energy 1998. 32 p. + app. 9 p. (unpublished)

2 Mangs Johan, Keski-Rahkonen Olavi. Full scale fire experiments on vertical and horizontal cable trays. VTT Publications 324. October 1997. 58 p. + app. 44 p.

3 Huhtanen R. Simulation of a smoke detector test. VTT Research report ENE21/8/98. VTT Energy 1998. 44 p. + app 3 p.

4 Björkman J, Keski-Rahkonen O. Response of fire detectors to different smokes. VTT Publications 295. Espoo 1997. 33 p.

5 Björkman J, Keski-Rahkonen O. Full scale experiments with different smokes. VTT Publications 332. Espoo 1997. 18 p. + app. 62 p.

6 Fluent User's Guide. Volumes 1–4. Version 4.4, Second edition, May 1997. Fluent Inc. Lebanon, New Hampshire, 1997.

7 Huhtanen R. Loviisan valvomorakennuksen kaapelitilan 1V1141 paloturvallisuusanalyysi. (Fire safety analysis of a cable room in the Loviisa power plant control building, Research report) Tutkimusselostus ENE 21/6/96. (in Finnish). VTT Energy 1996. 33 p. + app 4 p. (unpublished)

8 DiNenno P J et al (ed.). SFPE Handbook of fire protection engineering. National Fire Protection Association, Quincy, Massachusetts, Society of Fire Protection Engineers, Boston, Massachusetts. Second edition. 1995.

9 Bukowski R W, Averill J D. Methods for predicting smoke detector activation. Fire suppression and detection research application symposium, 25–27, 1998, Orlando, FL. Proceedings. National Fire Protection Research Foundation. pp. 64–72. (http://fire.nist.gov/fire/firedocs/bfrl98/bf98a.html)